Linear Observers Design for a Three-Pole Magnetic Bearing

Vinícius Ramos Vasco[1], Yago Pessanha Corrêa[2], Laura Julia Martins Mothé[3], Domingos de Farias Brito David[4], and Afonso Celso Del Nero Gomes[5]

[1] Marinha do Brasil (*Brazilian Navy*)
viniciusramosvasco@gmail.com
[2] Instituto Federal Fluminense (IFFluminense)
yago.correa@iff.edu.br
[3] Universidade Federal do Rio de Janeiro (UFRJ)
lauramothe@gmail.com
[4] Universidade Federal Fluminense (UFF)
domingos@vm.uff.br
[5] Universidade Federal do Rio de Janeiro (UFRJ)
nero@coep.ufrj.br

Abstract

In this work, linear observers for a three-pole active magnetic bearing (AMB) were designed and simulated, considering the AMB modelled as a linear dynamical system. Although the system being nonlinear, under the assumption of lower speeds, the linearized model can behave similarly to the nonlinear model. The linearized model was made from the reluctance forces equations and, as the system is naturally unstable, Linear Quadratic Regulator (LQR) was used to stabilize the system. The state vector contains both the horizontal and vertical sensor measurements, and also their derivatives, that are not measured. For the state feedback with LQR, it is necessary to have all the state vector data, and linear observers are a way to obtain the non-measured states. Observation errors for the full and reduced order linear observers are then compared.

1 Background

Active magnetic bearings are mechatronic devices that allow spinning rotors to operate contactless, providing the possibility to achieve high speeds with low bearing losses, with a controllable dynamic that can change the suspension's stiffness to different applications or states of operation [1]. Magnetic bearings are suitable for situations that demand the conditions mentioned above, as well as high efficiency, low maintenance and green operation, some examples are in turbomachinery, flywheel energy storage applications, machines in aerospace, and industries that require clean environments, like food and pharmaceutical industry [2].

The majority of magnetic bearings installed in industries uses the eight poles geometry, that produces four uncoupled magnetic fluxes to balance the rotor [3]. However, further research suggested other configurations, such as 4-pole and 3-pole, both with coupled magnetic fluxes. One way magnetic bearings can be modelled is through reluctance forces, and analytically is possible to verify that they have very strong nonlinearities in relation to the base current, the control current, the number of turns, the air gap and the rotor's positions. In [4], the reluctance forces from the 8-poles and 4-poles magnetic bearings were analytically obtained, linearized and compared.

The main advantages of the 3-pole AMB in comparison to other geometries is that it requires fewer actuators, has smaller remagnetization frequency resulting in lower iron losses and allows more space to place sensors and to dissipate heat, being very convenient for low-cost applications [5]. The main disadvantage is the higher complexity in the design and implementation of nonlinear controllers. One of the first studies proposed to overcome this problem was

[6], providing an exact linearization via feedback. Even though the techniques and the implementation of nonlinear controllers have been more feasible over the time, the study of linear control implementation are valid in some conditions, like constant and low rotor speed, and smaller rotor displacements.

Through the equations of motion and the relations between the linearized reluctance forces and control currents it is possible to model the system with rigid rotor and active magnetic bearings in the state-space form [4, 7]. The proper modelling allows to directly apply some techniques like state-space analysis with linear state-feedback, as well as optimal control and state observers, subjects discussed in detail in the control literature [8, 9, 10].

2 Discussion

This paper addresses the observation errors comparison of a three-pole magnetic bearing, modelled as a linear dynamical system with linear observers to estimate the states not measured. The responses using the full and reduced order observer will be compared. The 3-pole magnetic bearing considered is in the optimal configuration, as proposed in [5]. This optimal design considers the bearing supporting a rotor in a horizontal position and $\pi/6$ orientation, ensuring stability and base currents that minimizes the iron loss. Besides that, it also allows to reduce one actuator from the scheme by using only one coil wiring to the two upper poles, as shown in Figure 1.

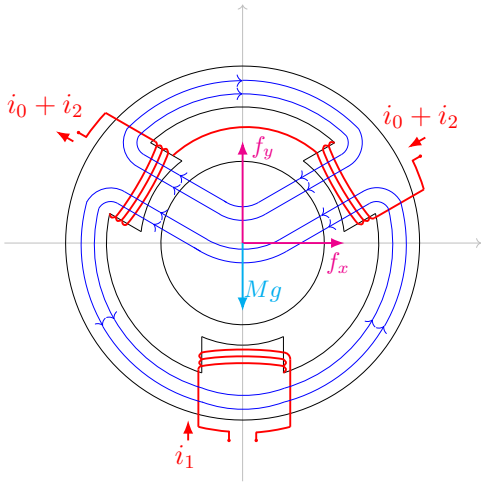

Figure 1: 3-Pole Magnetic Bearing in optimal design.

The stabilization problem in this work refers to control the differential currents in order to view how the rotor's center position changes over the time. As the region of study is close to the desired center point, linearization and linear control appears as valid tools for the analysis. Some examples of studies that have been made with the nonlinear control approach are in [11], [12] and [13]. For the linear approach, the detailed procedure on how to obtain the horizontal and vertical reluctance forces (f_x and f_y), here presented in (1), and how to model the system

using these equations are in [7][1]. The linearized reluctance forces for the 3-pole AMB are:

$$f_x = \frac{1}{2} g_p x + \frac{\sqrt{3}}{3} g_i i_1, \quad f_y = \frac{1}{2} g_p y + g_i i_2 \tag{1}$$

where

$$g_p = \frac{\mu_0 \ A \ n^2 \ i_0^2}{h^3}, \quad g_i = \frac{\mu_0 \ A \ n^2 \ i_0}{h^2}, \tag{2}$$

μ_0 is the permeability of free space, A is the pole's surface area, n is the coils turns number, h is the gap's size, i_0 is the coil base current, i_1 and i_2 are the coils differential currents, used as inputs to the rotor's position control.

The mechanical system model in state space for the 3-pole magnetic bearing considered the operation in a condition with disturbances, very close to what should be in a real condition. The external actions considered were the ones due to the torques from: the magnetic force, the gravitational force and the supporting bearing. Using the equations from the classic rotational dynamic and doing some algebrism, all detailed in [7] and [4], it is possible to set the model in state space form:

$$\dot{\boldsymbol{x}}(t) = A(\omega)\boldsymbol{x}(t) + B\boldsymbol{u}(t), \quad \boldsymbol{y} = C\boldsymbol{x} \tag{3}$$

in which matrices $A(\omega)$, B and C, the state vector $\boldsymbol{x}$ and the control inputs $\boldsymbol{u}$ are shown in (4), (5) and (6) :

$$A(\omega) = \begin{bmatrix} 0_2 & I_2 \\ K_1 I_2 & -G_e(\omega) \end{bmatrix}, \quad B = \begin{bmatrix} 0_2 \\ K_2 I_2 \end{bmatrix}, \tag{4}$$

$$C = \begin{bmatrix} I_2 & 0_2 \end{bmatrix}, \quad \boldsymbol{x} = \begin{bmatrix} x_s & y_s & \dot{x}_s & \dot{y}_s \end{bmatrix}^T, \tag{5}$$

$$\boldsymbol{u} = \begin{bmatrix} \frac{\sqrt{3}}{3} i_1 & i_2 \end{bmatrix}^T \tag{6}$$

where the constants K_1, K_2 depends on design parameters, the 2x2 matrix G_e depends on design parameters and also rotor speed, as shown in [7], the 0_2 is the 2x2 zero matrix, the I_2 is the 2x2 identity matrix, x_s and y_s are the sensors' displacement measurements.

This open loop model is unstable, as the state matrix has poles with positive real part, so a closed loop control is necessary to stabilize the system.

With the linearized model in state space form, it is very straightforward to verify that the system is observable, controllable, and the LQR is an option to stabilize the system, as this state feedback control can relocate the closed loop eigenvalues to have negative real parts. The LQR control in magnetic bearing has potential problems with robustness due to parameters uncertainties and instability with different speeds [1]. As in this work we consider the system with negligible modelling uncertainties and with constant rotational speed, LQR should be viable for analysis.

The performance index V for the infinite horizon LQR is the integral of two quadratic forms sum:

$$V(\boldsymbol{x}, \boldsymbol{u}, t_0) = \int_{t_0}^{\infty} (\boldsymbol{x}^T Q \boldsymbol{x} + \boldsymbol{u}^T R \boldsymbol{u}) dt, \tag{7}$$

where Q is a symmetric semi-positive definite matrix and R is symmetric positive definite. As the origin is considered the reference position ($\boldsymbol{r} = \boldsymbol{0}$), for this problem the LQR control input $\boldsymbol{u}$ is given by

$$\boldsymbol{u} = F\boldsymbol{x}, \tag{8}$$

[1] In this reference there are typos in equations (41), (51) and (67), the negative signs should be positive

where

$$F = -R^{-1}B^T P, \tag{9}$$

with P being the solution to the Algebric Ricatti Equation (ARE). The diagram for the LQR state feedback is shown in Figure 2.

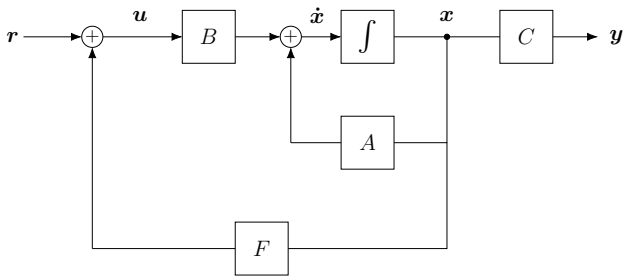

Figure 2: State feedback diagram.

But the implementation of the LQR control assumes that the states $\dot{x}_s$ and $\dot{y}_s$ are available, which usually is not the case. To obtain them, one option is to use sensors for direct measure, but it adds more cost to the set. The other option is to differentiate the signals of x_s and y_s, but with the inconvenience of amplifying the high frequency noise. In practical applications, digital computers are used, so the differentiation is obtained by subtracting the value of one sample to the value of one prior and dividing the result to the sample time. It is also common the use of filters to minimize the effect of noise. In this work we will design the full-order observer and the reduced-order observer theoretically and compare the simulated responses.

Both observers use the system's input and output to estimate the states [9], with the full order observer estimating all the states, regardless if they are already available or not, and the reduced-order observer estimating only the non-measured states. Then the estimated state vector $\hat{\boldsymbol{x}}$ is used to feedback to the system's input. For the full-order observer, the diagram is in Figure 3.

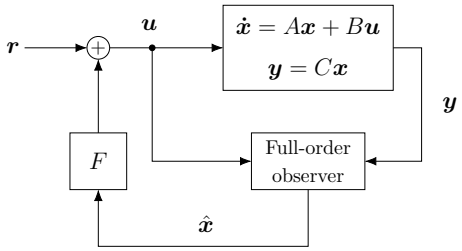

Figure 3: Estimated state feedback with full-order observer.

Detailing the Observer block in Figure 4, the full-order observer will contain a replica of the system matrices A, B and C, with the estimation error $\boldsymbol{e}$ being used by the replica system. The observer gain L must be chosen to allow $\boldsymbol{e}$ to exponentially decay to 0 for any error initial condition [14], and the observer dynamic also needs to be faster than the system dynamic. In this work we choose the eigenvalues of $A - LC$ to be 5 times faster than the closed-loop system eigenvalues.

As the system in study is fully controllable and observable, the separation principle allows to independently do the pole placement design and the observer design [9], as the extended

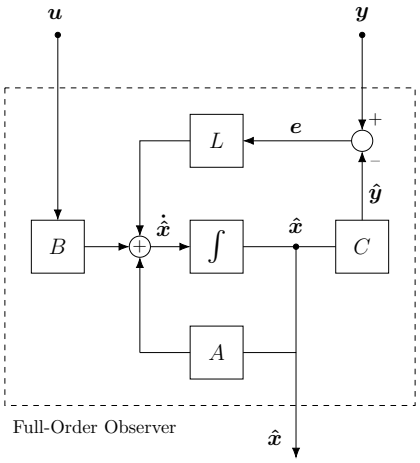

Figure 4: Detailed full-order observer block.

system equation is given by equation (10):

$$\begin{bmatrix} \dot{\boldsymbol{x}} \\ \dot{\boldsymbol{e}} \end{bmatrix} = \begin{bmatrix} A + BF & -BF \\ 0 & A - LC \end{bmatrix} \begin{bmatrix} \boldsymbol{x} \\ \boldsymbol{e} \end{bmatrix}, \tag{10}$$

where the estimation error $\boldsymbol{e}$ is the difference between the system output $\boldsymbol{y}$ and the estimation output $\hat{\boldsymbol{y}}$,

$$\boldsymbol{e} = \boldsymbol{y} - \hat{\boldsymbol{y}} = C(\boldsymbol{x} - \hat{\boldsymbol{x}}). \tag{11}$$

The reduced order observer allows estimating only the non-available states, by separating the state $\boldsymbol{x}$ and matrices A, B and C in two parts: the available part and the unavailable part, here identified with subindices a and u, respectively. The diagram for the state feedback with reduced order observer is presented in Figure 5.

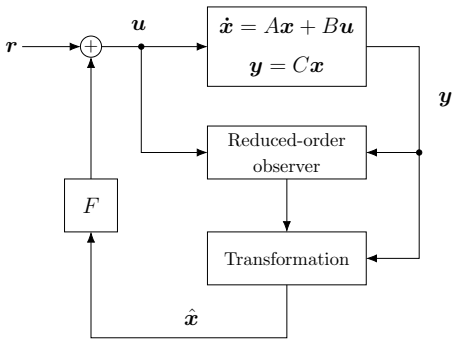

Figure 5: Estimated state feedback with reduced-order Observer.

Detailing the reduced-order observer and the transformation block in Figure 6, the matrices $\hat{A}, \hat{B}, \hat{C}, \hat{D}$ and $\hat{G}$ are expressions related to the available and unavailable parts of the system matrices as well as the observer gain for the reduced system, here given by L_r.

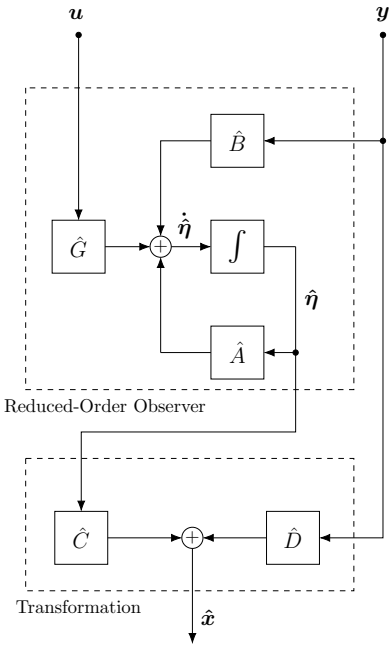

Figure 6: Detailed reduced-order Observer block and Transformation block.

Following [9], the dynamical system can be rewritten in the following form:

$$\dot{\boldsymbol{x}} = \begin{bmatrix} \dot{\boldsymbol{x}}_{\boldsymbol{a}} \\ \dot{\boldsymbol{x}}_{\boldsymbol{u}} \end{bmatrix} = \begin{bmatrix} A_{aa} & A_{au} \\ A_{ua} & A_{uu} \end{bmatrix} \begin{bmatrix} \boldsymbol{x}_{\boldsymbol{a}} \\ \boldsymbol{x}_{\boldsymbol{u}} \end{bmatrix} + \begin{bmatrix} B_a \\ B_u \end{bmatrix} \boldsymbol{u}, \tag{12}$$

$$\boldsymbol{y} = C \begin{bmatrix} \boldsymbol{x}_{\boldsymbol{a}} \\ \boldsymbol{x}_{\boldsymbol{u}} \end{bmatrix} = \begin{bmatrix} I_2 & 0_2 \end{bmatrix} \begin{bmatrix} \boldsymbol{x}_{\boldsymbol{a}} \\ \boldsymbol{x}_{\boldsymbol{u}} \end{bmatrix} = \boldsymbol{x}_{\boldsymbol{a}}. \tag{13}$$

The matrices $\hat{A}, \hat{B}, \hat{C}, \hat{D}$ and $\hat{G}$, indicated in Figure 6, are given by:

$$\hat{A} = A_{uu} - L_r A_{au}, \tag{14}$$

$$\hat{B} = \hat{A} L_r + A_{ua} - L_r A_{aa} \tag{15}$$

$$\hat{C} = \begin{bmatrix} 0_2 & I_2 \end{bmatrix}^T, \quad \hat{D} = \begin{bmatrix} I_2 & L_r \end{bmatrix}^T \tag{16}$$

$$\hat{G} = B_u - L_r B_a \tag{17}$$

The matrices $\hat{C}$ and $\hat{D}$ are necessary to reconstruct the full state with the available part coming from the output and the unavailable part coming from the reduced-order observer.

3 Results

The rotor speed initially considered for the simulation was $\omega = 356$ rad/s, the base current $i_0 = 0.23$ A, and the design parameters K_1, K_2 and G_e from equation (4) are given by:

$$K_1 = 3101.24, \quad K_2 = 19.76, \tag{18}$$

$$G_e = \begin{bmatrix} 0.51 & 10.22 \\ -10.22 & 0.51 \end{bmatrix}. \tag{19}$$

For $Q = I_4$ and $R = I_2$, the feedback gain matrix F is given by:

$$F = \begin{bmatrix} 311.27 & 28.24 & 5.68 & 0 \\ -28.24 & 311.27 & 0 & 5.68 \end{bmatrix}, \tag{20}$$

and the system's closed-loop eigenvalues are $-46.45 \pm j4.21$ and $-66.2 \pm j6.01$.

A simulation was made to compare the responses for the nonlinear model when subjected to the same linear control used by the linear model, to evaluate if the responses were similar. The schemes used are shown in Figure 7.

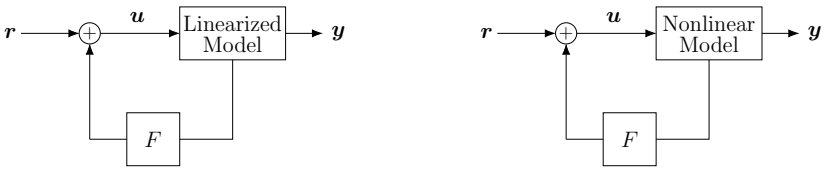

Figure 7: LQR control applied to the linearized and nonlinear model

The differences between the linearized and the nonlinear control responses depends on the rotor speed. They are negligible when $\omega = 356$ rad/s, as can be seen in Figure 8a, but for $\omega = 3204$ rad/s, for example, the differences become significant, as can be seen in Figure 8b.

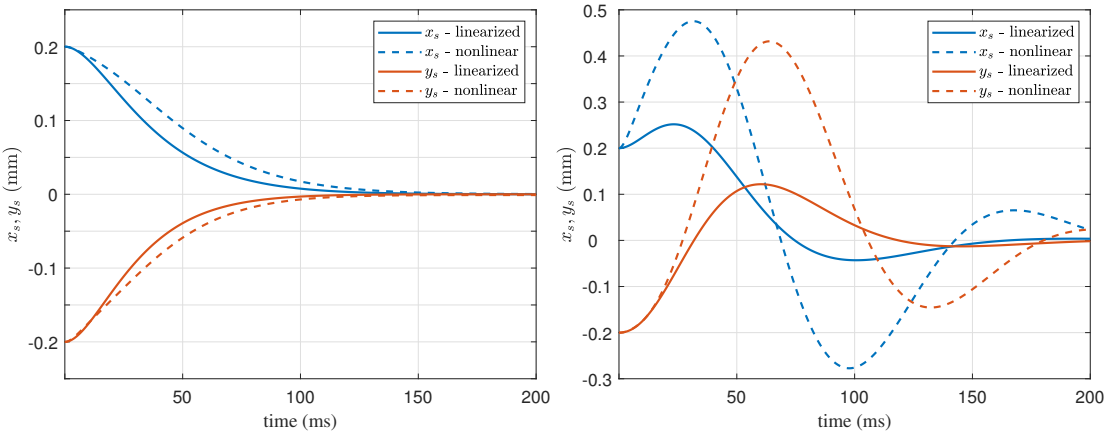

(a) When $\omega = 356$ rad/s

(b) When $\omega = 3204$ rad/s

Figure 8: LQR Outputs to the linearized and nonlinear models

For the linearized system with rotor speed $\omega = 356$ rad/s, the full-order observer gain L was designed considering the observer eigenvalues 5 times faster than the closed-loop system

eigenvalues, resulting in

$$L = \begin{bmatrix} 580.20 & -21.77 \\ -8.33 & 545.49 \\ 8.59 \times 10^4 & -6.14 \times 10^3 \\ 2.65 \times 10^3 & 7.49 \times 10^4 \end{bmatrix}. \tag{21}$$

For an initial condition $x_0 = \begin{bmatrix} 0.2 & -0.2 & 0 & 0 \end{bmatrix}^T$ and an observer initial condition $x_{0-obs} = \begin{bmatrix} 0 & 0 & 0 & 0 \end{bmatrix}^T$, the observation error for each state of the full order observer is presented in Figure 9a.

As for the reduced-order observer design, the observer gain L_r was designed considering the eigenvalues of the unobservable part being 5 times faster than the eigenvalues of the observable part, resulting in:

$$L_r = \begin{bmatrix} 231.75 & -10.22 \\ 10.22 & 231.75 \end{bmatrix}. \tag{22}$$

From equations (14), (15), (16) and (17), the reduced-order observer matrices $\hat{A}, \hat{B}, \hat{C}, \hat{D}$ and $\hat{G}$ are:

$$\hat{A} = \begin{bmatrix} -232.26 & 0 \\ 0 & -232.26 \end{bmatrix}, \tag{23}$$

$$\hat{B} = 10^4 \times \begin{bmatrix} -5.07 & 0.24 \\ -0.24 & -5.07 \end{bmatrix} \tag{24}$$

$$\hat{C} = \begin{bmatrix} 0_2 & I_2 \end{bmatrix}^T, \quad \hat{D} = \begin{bmatrix} I_2 & L_r \end{bmatrix}^T, \tag{25}$$

$$\hat{G} = \begin{bmatrix} 19.76 & 0 \\ 0 & 19.76 \end{bmatrix}, \tag{26}$$

and the corresponding observation errors for each state, for the same initial conditions mentioned above are shown in Figure 9b.

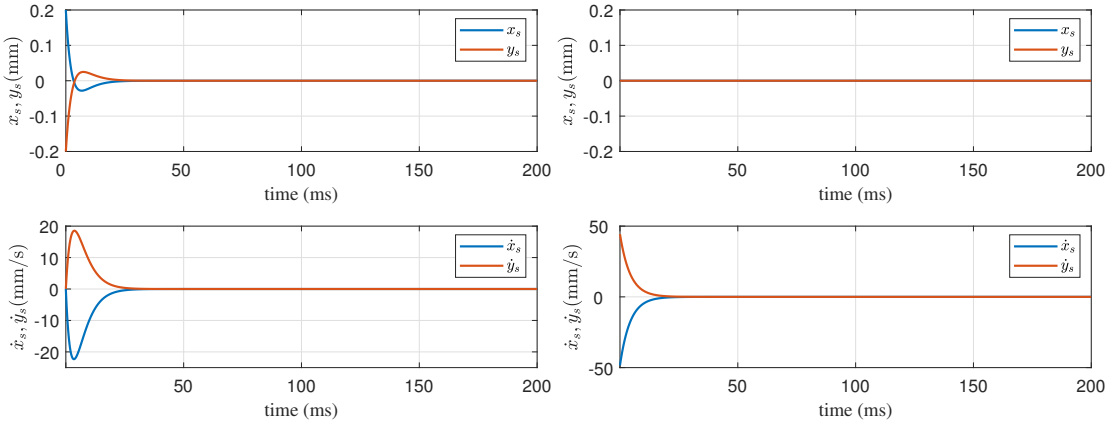

(a) full-order (b) reduced-order

Figure 9: Observation errors when $\omega = 356$ rad/s

In the noiseless conditions simulated, the reduced-order observer presented slightly better transient response performance over the full-order observer, with observation errors for the non-measured states about 5 ms faster than the full-order observation errors. In noisy environment,

it is expected to see fewer advantages from the reduced-order observer due to more non-limited bandwidth noise in x_u [10], partly because of the memoryless transformation of y. It was not seen differences in estimation errors from figures 9a and 9b when simulating with speeds lower $\omega = 1780$ rad/s, approximately. For larger speeds, the difference between the nonlinear and linear outputs become significant, and the linear model isn't a good approximation.

4 Conclusions

We have shown how to design linear Luenberger observers for the 3-pole active magnetic bearing. The use of observers in magnetic bearings applications was considered because they can be modelled as a linear dynamical system via linearization of the reluctance forces. Both the full-order and the reduced-order observers could estimate the non-available states in close times, with the full-order observer in about 20 ms and the reduced-order observer in 15 ms, although it had larger initial error than the full-order. The shaft's rotation speed affected the linearized model performance, with it being very close to the nonlinear model for lower speeds, until about $\omega = 1780$ rad/s. For larger speeds, the linearized model responses have larger differences to the nonlinear model responses. This analysis shows that the use of the observers with the linearized model is suitable for problems where the application doesn't require very high speeds. More studies involving observers and digital differentiation in magnetic bearings will be done in future work.

References

[1] G. Schweitzer, H. Bleuler, E. H. Maslen, M. Cole, P. Keogh, R. Larsonneur, E. Maslen, R. Nordmann, and Y. Okada, *Magnetic Bearings: Theory, Design, and Application to Rotating Machinery.* : Springer Berlin Heidelberg, 2009.

[2] A. Chiba, T. Fukao, O. Ichikawa, M. Oshima, M. Takemoto, and D. G. Dorrell, *Magnetic Bearings and Bearingless Drives.* : Elsevier, 1 ed., 2005.

[3] W. Zhang and H. Zhu, "Radial magnetic bearings: An overview," *Results in Physics*, vol. 7, pp. 3756–3766, 2017.

[4] D. F. B. David, J. A. Santisteban, and A. C. D. N. Gomes, "Modeling and Testing Strategies for an Interconnected Four-Pole Magnetic Bearing," *Actuators*, vol. 6, SEP 2017.

[5] S. Chen and C. Hsu, "Optimal design of a three-pole active magnetic bearing," *IEEE Transactions on Magnetics*, vol. 38, pp. 3458–3466, SEP 2002.

[6] C. T. Hsu and S. L. Chen, "Exact linearization of a voltage-controlled 3-pole active magnetic bearing system," *IEEE Transactions on Control Systems Technology*, vol. 10, pp. 618–625, JUL 2002.

[7] V. R. Vasco, A. C. D. N. Gomes, D. d. F. B. David, and J. A. Santisteban, "Considerations on the mechanical dynamics of interconnected flux three-pole magnetic bearings," in *Proceedings of ISMB16*, p. 8, 2018.

[8] T. Kailath, *Linear Systems.* Pearson Education (US), 1979.

[9] K. Ogata, *Modern Control Engineering.* : Prentice Hall, fifth edition ed., 2010.

[10] B. D. O. Anderson and J. B. Moore, *Optimal Control: Linear Quadratic Methods (Dover Books on Engineering).* : Dover Publications, Inc., 1990.

[11] C.-T. Hsu and S.-L. Chen, "Nonlinear control of a 3-pole active magnetic bearing system," *Automatica*, vol. 39, no. 2, pp. 291 – 298, 2003.

[12] S.-L. Chen, "Nonlinear Smooth Feedback Control of a Three-Pole Active Magnetic Bearing System," *IEEE Transactions on Control Systems Technology*, vol. 19, pp. 615–621, MAY 2011.

[13] S. M. Darbandi, M. Behzad, H. Salarieh, and H. Mehdigholi, "Linear Output Feedback Control of a Three-Pole Magnetic Bearing," *IEEE-ASME Transactions on Mechatronics*, vol. 19, pp. 1323–1330, AUG 2014.

[14] V. Radisavljevic-Gajic, "Linear observers design and implementation," in *Proceedings of the 2014 Zone 1 Conference of the American Society for Engineering Education*, IEEE, apr 2014.